

VI. Concluding Remarks

The results of our study indicate that the structural aspects of the reaction of singlet silylene with H_2 are very similar to the analogous reaction of singlet methylene. The reaction proceeds in two steps: the first electrophilic step leads to the transition state with one Si-H bond almost formed, whereas in the second nucleophilic step the product SiH_4 is reached. On the basis of the VBCM model,¹⁹ it was assumed that for the formation of the transition state, the reactants must be promoted to a valence state which can be *formally* visualized as the two reactants in their respective triplet states coupled to a singlet. With this assumption, the existence of an activation energy in the silylene reaction in contrast to methylene could be explained. We want to stress that the notion of a triplet valence state should not mean that the reaction really proceeds via the triplet state as was conjectured by Bell and co-workers.¹⁷ Such a mechanism would imply a nonadiabatic reaction, including an intersystem crossing step and therefore, would render the reaction highly improbable. The results of our calculations, however, indicate the possibility of an adiabatic course of the reaction, together with a modest activation energy.

From our proposed reaction mechanism, further conclusions can be drawn concerning the reactions of singlet silylene with substrates other than hydrogen. We traced the activation energy to the promotion energy needed to form the transition state, and we may anticipate that in other systems less energy is necessary

for that process. This is probably the case in the reaction of silylene with silane to disilane, where the low activation energy of 3 ± 3 kcal/mol¹⁰ is estimated. For the addition of silylene to ethylene, one can safely assume that the promotion energy to a valence state of the ethylene will be much lower than that for hydrogen. Concomitantly, Anwari and Gordon,⁸ from their calculations for this reaction, find no activation energy. Finally, the reaction mechanism proposed above allows us to predict a higher activation energy for the reaction of GeH_2 with hydrogen since the singlet-triplet separation of this behavior analogue to SiH_2 is higher by about 4 kcal/mol.³⁴

Acknowledgment. Many discussions with Drs. P. Potzinger and B. Reimann are gratefully acknowledged. G.O. expresses his gratitude to Prof. Dr. P. Durand for the use of his pseudopotential method. Thanks are also due to Prof. Dr. R. J. Buenker for making available a copy of the MRD-CI program system. All calculations have been performed at the computing center of the Max-Planck-Institut für Strahlenchemie (Dr. E. Ziegler). A. S. thanks Prof. Dr. A. Janoschek and G.O. Prof. Dr. O. E. Polansky for continuing support. Critical reading of the manuscript by Prof. Dr. J. N. Silverman is gratefully acknowledged.

Registry No. SiH_2 , 13825-90-6; SiH_4 , 7803-62-5; H_2 , 1333-74-0.

(34) Olbrich, G., unpublished results.

Spontaneous and Induced Homolysis of Bis(triphenylphosphine)octacarbonyldimanganese(*Mn-Mn*)

Anthony Poë* and Chandra V. Sekhar

Contribution from the J. Tuzo Wilson Laboratories, Erindale College, University of Toronto, Mississauga, Ontario, Canada L5L 1C6. Received June 1, 1984

Abstract: Kinetic studies show that the complex $Mn_2(CO)_8(PPh_3)_2$ reacts thermally by two paths with $C_2H_2Cl_4$, $C_{16}H_{33}I$, O_2 , NO , $P(OEt)_3$, and $P-n-Bu_3$ in decalin or cyclohexane. Reactions with CO or $P(OPh)_3$ proceed only by one of these paths. The two paths are of approximately equal importance and both show a very close fit to the same, rather complex, form of rate equation. The equation is quite inconsistent with any form of rate-determining dissociation, but it is consistent with two forms of reversible homolysis, one spontaneous and one induced. The latter involves initial, reversible formation of a reactive isomer of $Mn_2(CO)_8(PPh_3)_2$ which undergoes homolysis when attacked by a sufficiently reactive reagent. Both paths are therefore operative in reactions with the more reactive reagents, but reactions with CO and $P(OPh)_3$ proceed only via spontaneous homolysis because these reagents are evidently unable to induce homolysis of the reactive isomer of the complex. A possible structure for the reactive isomer is one formed by metal migration, i.e., it can be formulated as $(Ph_3P)(OC)_4Mn(\mu-CO)Mn(CO)_3(PPh_3)$ which contains a bridging CO ligand, no $Mn-Mn$ bond, and a vacant coordination site on one Mn atom. Attack at this site by suitably active reagents is postulated to lead to fragmentation. These results show that behavior previously thought to be uniquely indicative of spontaneous homolysis could also be explained by reversible homolysis induced by the reactant after isomerization of the complex. Rate constants are derived for halogen transfer from $C_2H_2Cl_4$ or $C_{16}H_{33}I$ to $\cdot Mn(CO)_4(PPh_3)$ and for nucleophilic displacement of PPh_3 from $\cdot Mn(CO)_4(PPh_3)$ by $P(OPh)_3$, $P(OEt)_3$, and CO .

Thermally induced homolysis of the metal-metal bonds in dinuclear metal carbonyls would, if it occurred, be a very useful phenomenon. It would allow activation enthalpies to be obtained for homolysis, and these would provide less ambiguous and more precise quantitative estimates of the strengths of the metal-metal bonds than are available by using other methods.¹ At first sight, the occurrence of initial homolysis should be demonstrable by kinetic methods. When the homolysis is reversible, reactions should change smoothly from being first order to half order in [complex] as the homolysis becomes more and more easily reversed.¹ This will generally be the case as the concentration of

the complex is increased. Such kinetic behavior has been observed for the thermal decomposition reactions of $Mn_2(CO)_{10}$,² $Re_2(CO)_{10}$,³ $Tc_2(CO)_{10}$,⁴ $MnRe(CO)_{10}$,² and $Mn_2(CO)_8[P(OPh)_3]_2$ ⁵ in the presence of oxygen, and it was proposed that initial reversible homolysis was indeed the dominant mechanism for decomposition reactions of these complexes, and for substitution and other reactions as well.

(2) Fawcett, J. P.; Poë, A. J.; Sharma, K. R. *J. Am. Chem. Soc.* **1976**, *98*, 1401-1407.

(3) Fawcett, J. P.; Poë, A. J.; Sharma, K. R. *J. Chem. Soc. Dalton Trans.* **1979**, 1886-1890.

(4) Fawcett, J. P.; Poë, A. J. *J. Chem. Soc., Dalton Trans.* **1976**, 2039-2044.

(5) Chowdhury, D. M.; Poë, A. J.; Sharma, K. R. *J. Chem. Soc., Dalton Trans.* **1977**, 2352-2355.

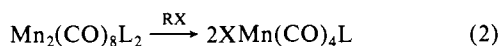
(1) (a) Poë, A. J. *ACS Symp. Ser.* **1981**, *155*, 135-166. (b) Poë, A. J. *Chem. Br.* **1983**, *19*, 997-998, 1001-1003.

Although some arguments were presented⁶ against this being so, no clear experimental evidence against homolysis⁷ was obtained until recently.⁸⁻¹⁰ It was found⁸ that $Mn_2(CO)_{10}$ and $Re_2(CO)_{10}$ failed to undergo a scrambling reaction under conditions such that it should have been observed if homolysis were occurring as claimed. Subsequently, isotopic labeling methods were used to show that thermal homolysis of $Re_2(CO)_{10}$ ⁹ and $Mn_2(CO)_{10}$ ¹⁰ individually does not occur in the absence of any reactants and homolysis of the Re-Re bond does not occur in reactions of PPh_3 with $Re_2(CO)_9(PPh_3)$ or $Re_2(CO)_8(PPh_3)_2$.⁹ Scrambling between $Mn_2(CO)_{10}$ and $Re_2(CO)_{10}$ has now been shown to occur, under forcing conditions, via aggregation to form tetranuclear intermediates rather than via fragmentation.¹¹

It has, therefore, become necessary to determine what mechanism other than initial reversible homolysis could give rise to the peculiar kinetic behavior found for the decomposition reactions of the decacarbonyls, and also to discover which of their substituted derivatives, if any, undergo spontaneous homolysis. The substitution reaction 1 shows complicated kinetic behavior that is

$$Mn_2(CO)_8(PPh_3)_2 + P(OPh)_3 \rightarrow Mn_2(CO)_8(PPh_3)P(OPh)_3 + PPh_3 \quad (1)$$

entirely consistent with initial homolysis and quite incompatible with any simple ligand dissociative process.¹² In addition, the reactions shown in eq 2 ($RX = 1,1,2,2$ -tetrachloroethane; $L = PPh_3$, $P-n-Bu_3$, and $P(C_6H_{11})_3$) proceed quantitatively at the same



limiting rate as thermal decomposition under O_2 .¹³ When $L = PPh_3$, the rates decrease below the limiting rate as $[C_2H_2Cl_4]$ is decreased, showing that some form of reactive intermediate is generated that can competitively react with $C_2H_2Cl_4$ or revert to $Mn_2(CO)_8(PPh_3)_2$. These observations all suggest that thermal reactions with halocarbons should be able to provide evidence for homolysis in the same way as the corresponding photochemical reactions are believed to.¹⁴ We have therefore undertaken a study of the kinetics of reactions of such complexes with selected halocarbons. We report here results for reactions of $Mn_2(CO)_8(PPh_3)_2$, taken as a model complex, with $C_2H_2Cl_4$ and $I-n-C_{16}H_{33}$ and have extended the study of reactions such as (1) to include those with $P(OEt)_3$ and $P-n-Bu_3$. We also report a study of relevant scrambling reactions.

Experimental Section

The complex $Mn_2(CO)_8(PPh_3)_2$ was prepared in high yield from $Mn_2(CO)_{10}$ (Strem Chemicals, Inc.; 300 mg, 0.77 mmol) by reaction with PPh_3 (BDH; 2.53 g, 10 mmol) in degassed decalin (Aldrich; 15 mL) at 170 °C for 15–20 min under a partial vacuum. Dark orange crystals separated after cooling overnight and were recrystallized from CH_2Cl_2 -MeOH mixtures. The complex was characterized by its melting point (187 °C; cf. 189–190 °C¹⁵), its IR absorption¹⁶ at 1960 cm^{-1} (ϵ

20000 $M^{-1} cm^{-1}$), and its UV-vis absorption¹⁶ at 376 nm (ϵ 31000 $M^{-1} cm^{-1}$), both spectra measured in decalin. $Mn_2(CO)_8(P-n-Bu_3)_2$ was prepared and characterized by published methods.^{13,15} $C_2H_2Cl_4$ (BDH) was distilled and dried over molecular sieves before use. $C_{16}H_{33}I$ (ICN Pharmaceuticals, Inc.) was used as received. $P(OEt)_3$ (Eastman Kodak) was distilled over sodium, and $P-n-Bu_3$ (Strem Chemicals) was distilled over sodium under reduced pressure. Decalin was distilled¹¹ and stored under argon over molecular sieves. CO was "Linde" Specialty Grade (Union Carbide of Canada, Ltd.).

Solutions for kinetic study were made up by heating degassed suspensions of $Mn_2(CO)_8(PPh_3)_2$ under vacuum in a Schlenk tube with a hot air drier for a few minutes until the solutions were clear. Most samples were made up in the presence of sufficient PPh_3 to give a final value of $[PPh_3] = 0.06 M$ in the reactant solutions, and this served to minimize decomposition of the complex during dissolution.^{16a} The Schlenk tubes were then charged with argon or other appropriate gas and immersed in a thermostat bath (Brinkman-Lauda Model K), the samples being completely shielded from laboratory light. The requisite reactant, in solution if appropriate, was then injected by syringe in known amounts through the septum cap sealing the Schlenk tube. After the mixture was shaken well and the temperature allowed to equilibrate, solutions were withdrawn by syringe at regular intervals for spectroscopic measurement either immediately or after storing in small sealed vials kept on ice in the dark until the run was complete. Initial concentrations were estimated from measurements of absorbance combined with the known molar absorption coefficients. The solutions were shown to obey Beer's law over the range of concentrations used. The pressure of gas in the Schlenk tube was maintained after each sample withdrawal. Temperatures of reactant solutions were estimated by measuring the temperature of decalin in a Schlenk tube placed in the same position in the bath as the reaction tube just before and after a run. The temperatures were measured with an iron-Constantan thermocouple inserted through a rubber septum cap and connected to a digital multimeter (Data Precision Model 3500). Temperatures were maintained constant to within ± 0.1 °C.

Reactions with $C_2H_2Cl_4$ and $C_{16}H_{33}I$ were generally followed by measuring the decreasing absorption of the band due to $Mn_2(CO)_8(PPh_3)_2$ at 1960 cm^{-1} . Final absorbances were about 20% of initial absorbances, and plots of $\ln(A_t - A_\infty)$ against time were generally linear for at least 1–1.5 half-lives. The initial gradients were taken as measurements of k_{obsd} , the observed apparent pseudo-first-order rate constants characteristic of a particular initial concentration, C , of complex. The IR spectra of the products were characteristic of *cis*- $XMn(CO)_4(PPh_3)_2$ for faster reactions, but the slower runs showed some formation of *fac*- $XMn(CO)_3(PPh_3)_2$ due to subsequent reaction of the initial product when free PPh_3 was present.¹³ Reaction with $C_2H_2Cl_4$ is known to be essentially quantitative,¹³ and the same is assumed to be the case for reaction with $C_{16}H_{33}I$. No spectroscopic evidence was observed for any side products, and there was no evidence for decomposition.

Reactions with $P(OEt)_3$ were carried out in the absence of PPh_3 and proceeded cleanly to form $Mn_2(CO)_8(PPh_3)P(OEt)_3$ as evidenced by the strong IR band that grew in at 1962 cm^{-1} and the intense maximum in the electronic spectrum at 364 nm. These are intermediate between the spectra of $Mn_2(CO)_8(PPh_3)_2$ and $Mn_2(CO)_8P(OEt)_3$, the latter showing absorptions at 1966 cm^{-1} ¹⁵ and 350 nm.¹³ The kinetics were followed by monitoring changes in the absorbance at 376 nm which, because of a decrease in intensity as well as the slight shift in the maximum, were more pronounced than the changes in the IR spectra. The product was quite stable under the conditions of the reaction, and good values of A_∞ were obtained, the decrease of absorbance being ca. 60% during the course of the reaction.

Reactions with $P-n-Bu_3$ were accompanied by the growth of an IR band at 1953 cm^{-1} and a UV-vis band at 365 nm. Subsequent slower reaction led to bands at 1947 cm^{-1} and 357 nm characteristic^{13,17} of $Mn_2(CO)_8(P-n-Bu_3)_2$. The initial product can therefore be concluded to be $Mn_2(CO)_8(PPh_3)(P-n-Bu_3)$. The UV-vis spectra were not suitable for monitoring the reactions because of the overlapping second stage, and they were therefore followed by measuring the decreasing absorbance of the well-separated band of the reactant complex at 1960 cm^{-1} . Pseudo-first-order rate plots were linear for at least 1–1.5 half-lives for both substitution reactions.

Results and Discussion

The Rate Equation. Reactions with $C_2H_2Cl_4$ and $C_{16}H_{33}I$ increase in rate with increasing $[RX]$ until a limiting rate is reached that is the same for both halocarbons. Reactions that

(6) Sonnenberger, D.; Atwood, J. D. *J. Am. Chem. Soc.* **1980**, *102*, 3484–3489; *Inorg. Chem.* **1981**, *20*, 4031–4032.

(7) Poë, A. J. *Inorg. Chem.* **1981**, *20*, 4029–4031, 4032–4033.

(8) Schmidt, S. P.; Troglor, W. C.; Basolo, F. *Inorg. Chem.* **1982**, *21*, 1698–1699.

(9) Stolzenberg, A. M.; Muetterties, E. L. *J. Am. Chem. Soc.* **1983**, *105*, 822–827.

(10) Coville, N. J.; Stolzenberg, A. M.; Muetterties, E. L. *J. Am. Chem. Soc.* **1983**, *105*, 2499–2500.

(11) Marcomini, A.; Poë, A. J. *J. Am. Chem. Soc.* **1983**, *105*, 6952–6958.

(12) Fawcett, J. P.; Jackson, R. A.; Poë, A. J. *J. Chem. Soc., Dalton Trans.* **1978**, 789–793.

(13) Jackson, R. A.; Poë, A. J. *Inorg. Chem.* **1978**, *17*, 997–1003.

(14) (a) Geoffroy, G. L.; Wrighton, M. S. "Organometallic Photochemistry"; Academic Press: New York, 1979; Chapter 2. (b) Laine, R. M.; Ford, P. C. *Inorg. Chem.* **1977**, *16*, 388–391. (c) Fox, A.; Poë, A. J. *J. Am. Chem. Soc.* **1980**, *102*, 2497–2499.

(15) Osborne, A. G.; Stiddard, M. H. B. *J. Chem. Soc.* **1964**, 634–636.

(16) (a) Fawcett, J. P.; Poë, A. J. *J. Chem. Soc., Dalton Trans.* **1977**, 1302–1306. (b) An experiment reported in ref 16a seemed to show that reaction with O_2 was reduced in rate by CO to that characteristic of CO alone and with formation of $Mn_2(CO)_8(PPh_3)$ in high yield. Attempts to repeat this observation have failed. CO and O_2 were passed through reactant solutions at roughly equal rates. Rate constants obtained were the same as those for O_2 alone, and decomposition was the only reaction observed.

(17) Lewis, J.; Manning, A. R.; Miller, J. R. *J. Chem. Soc. A* **1966**, 845–854.

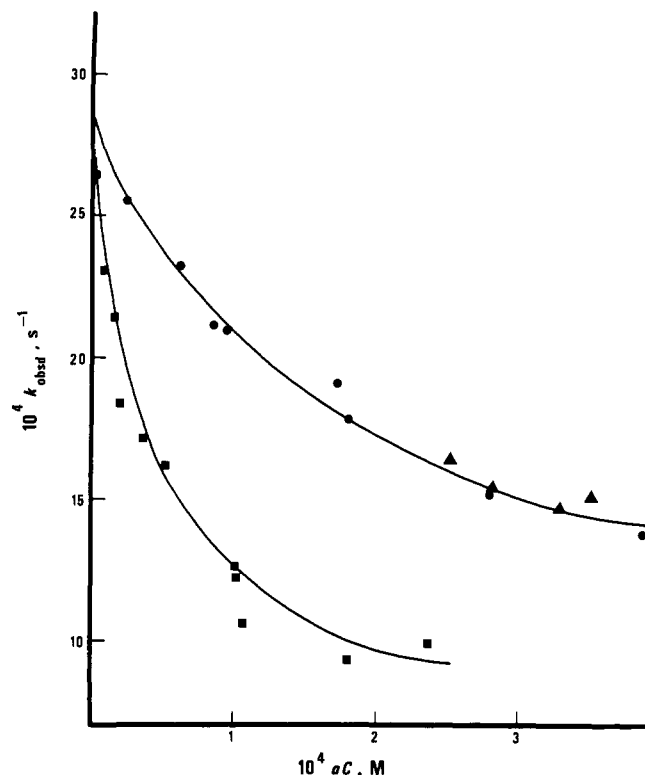


Figure 1. Dependence of k_{obsd} at 49.9 °C on the concentration, C , of $\text{Mn}_2(\text{CO})_8(\text{PPh}_3)_2$. (●) $[\text{C}_{16}\text{H}_{33}\text{I}] = 1.9 \times 10^{-3}$ M, $10^6 C = 25 - 388$ M, $[\text{PPh}_3] = 0.06$ M, reaction under Ar, $a = 1$. (▲) $[\text{C}_{16}\text{H}_{33}\text{I}] = 1.9 \times 10^{-3}$ M, $[\text{PPh}_3] = 0.10$ M, reaction solution equilibrated with CO, $a = 1$. (■) $[\text{C}_2\text{H}_2\text{Cl}_4] = 9.8 \times 10^{-3}$ M, $[\text{PPh}_3] = 0.06$ M, $10^6 C = 3.5 - 163$ M, reaction under Ar, $a = 1.45$. Continuous lines are calculated by means of eq 3 and the parameters given in Table I.

proceed at rates less than the limiting one show a dependence of k_{obsd} on initial concentrations, C , of complex (Figure 1) as well as on $[\text{RX}]$, and all the data show an excellent fit to eq 3. This is illustrated in Figure 2 for reaction with $\text{C}_{16}\text{H}_{33}\text{I}$, the intercept and gradient corresponding to the empirical rate constants k_a and k_b respectively.

$$k_{\text{obsd}} = k_a - k_b C k_{\text{obsd}}^2 / [\text{RX}]^2 \quad (3)$$

A similar plot is also obtained for reaction with the other halocarbon, $\text{C}_2\text{H}_2\text{Cl}_4$, but an alternative plot, based on the rearranged form of eq 3 shown in eq 4, is also strictly linear (Figure 3) when k_a is taken as the limiting value of k_{obsd} at high $[\text{C}_2\text{H}_2\text{Cl}_4]$ and low C . The values of k_{obsd} for reaction with $\text{P}(\text{OEt})_3$ also fit

$$(k_a - k_{\text{obsd}})^{1/2} / k_{\text{obsd}} = k_b^{1/2} C^{1/2} / [\text{RX}] \quad (4)$$

on an excellent straight line (Figure 2) according to eq 3, with $[\text{RX}]$ replaced by $[\text{P}(\text{OEt})_3]$. Reaction with $\text{P-}n\text{-Bu}_3$ was followed at such concentrations of $\text{P-}n\text{-Bu}_3$ that only limiting rates were obtained. Values of k_a and k_b (if obtained) for all these reactions are shown in Table I, together with values of k_a for reactions with O_2 and NO .¹⁵ Uncertainties in k_a and k_b , and values of $\sigma(k_{\text{obsd}})$, were estimated as described elsewhere.¹²

Apart from the excellent linearity of the plots in Figures 2 and 3, and the excellent fit of the data to the calculated line in Figure 1, an important feature is that data for reactions with halocarbons, carried out in the presence of different concentrations of PPh_3 and under CO, all fit exactly to eq 3 and 4. Figure 1 shows that k_{obsd} for reaction of 1.9×10^{-3} M $\text{C}_{16}\text{H}_{33}\text{I}$ with ca. 3×10^{-4} M complex, under Ar and at $[\text{PPh}_3] = 0.06$ M, is almost a factor of 2 lower than the limiting rate constant found at very low concentration of complex. If the rate-determining step were reversible dissociation of a PPh_3 ligand, there could be no dependence of k_{obsd} on $[\text{complex}]$ when $[\text{PPh}_3] \gg [\text{complex}]$ and constant. This is contrary to what is observed. Also, any increase

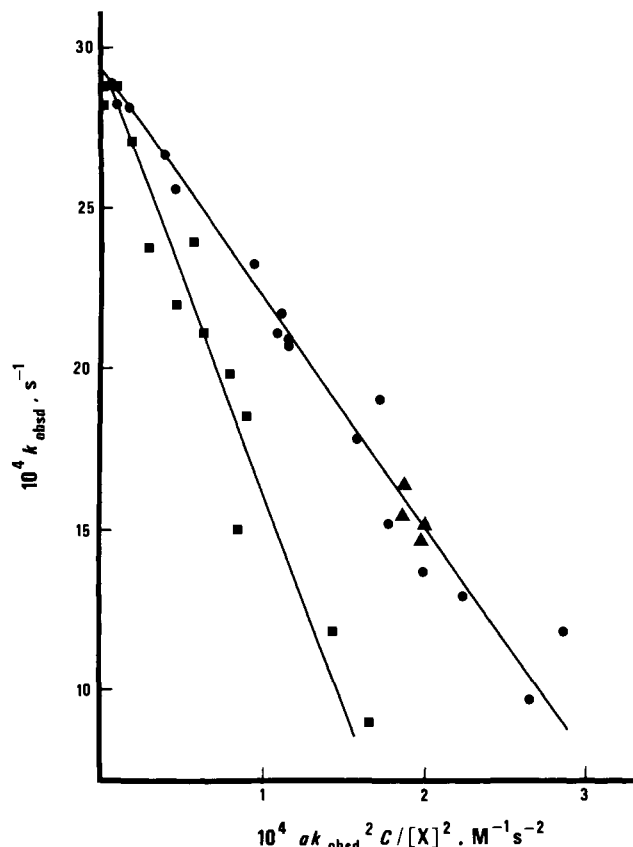


Figure 2. Dependence of k_{obsd} at 49.9 °C on $Ck_{\text{obsd}}^2/[\text{X}]^2$. (●) Reaction with $[\text{X}] = [\text{C}_{16}\text{H}_{33}\text{I}] = (0.7 - 320) \times 10^{-3}$ M under Ar, $10^6 C = 25 - 388$ M, $[\text{PPh}_3] = 0.06$ M, $a = 1$. (▲) Reaction with $[\text{X}] = [\text{C}_{16}\text{H}_{33}\text{I}] = 1.9 \times 10^{-3}$ M under CO, $[\text{PPh}_3] = 0.10$ M, $a = 1$. (■) Reaction with $[\text{X}] = [\text{P}(\text{OEt})_3] = (5 - 400) \times 10^{-3}$ M under Ar, $10^6 C = 13 - 177$ M, $[\text{PPh}_3] = 0$, $a = 3$.

Table I. Kinetic Data for Reactions of $\text{Mn}_2(\text{CO})_8(\text{PPh}_3)_2$

Reactant	T , °C	$10^4 k_a$, ^a s ⁻¹	k_b , ^a M s	$\sigma(k_{\text{obsd}})$, ^a %
CO^b	49.9	17.5 ± 0.2		3.5
$\text{P}(\text{OEt})_3^c$	49.9	17.5 ± 0.8	35 ± 7	5.5
O_2^b	49.9	32.0 ± 0.4		5.3
$\text{C}_{16}\text{H}_{33}\text{I}^d$	49.9	29.2 ± 0.4	7.1 ± 0.4	3.0
$\text{C}_2\text{H}_2\text{Cl}_4^d$	49.9	29.7 ± 0.7	$(1.5 \pm 0.2) \times 10^3$	7.6
$\text{P-}n\text{-Bu}_3^d$	49.9	28.4 ± 0.3^e		
$\text{P}(\text{OEt})_3^d$	49.9	29.2 ± 0.6	41.0 ± 1.3	4.4
$\text{P}(\text{OEt})_3^c$	39.9	4.20 ± 0.09	159 ± 10	7.6
O_2^b	39.9	7.23 ± 0.12		4.1
$\text{P-}n\text{-Bu}_3^d$	40.0	7.60 ± 0.8^e		
$\text{P}(\text{OEt})_3^d$	40.0	7.46 ± 0.14		
NO^b	40.0	7.4		
$\text{P}(\text{OEt})_3^f$	51.0	18 ± 2	ca. 1×10^4	
$\text{P-}n\text{-Bu}_3^f$	51.0	28 ± 1		

^aUncertainties in k_a and k_b are standard deviations (probable errors) estimated approximately, as described in ref 12, when derived from eq 3. The values of $\sigma(k_{\text{obsd}})$ are given by values of $100[\Sigma\{(k_{\text{obsd}} - k_{\text{calc}})/k_{\text{calc}}\}^2 / (N - 1)]^{1/2}$ where values of k_{calc} were obtained by using eq 3 and the listed value of k_a and k_b . N is the number of measurements of k_{obsd} . Allowance is made for the number of degrees of freedom, $N - 2$, so that 95% confidence limits can be obtained by doubling the estimated standard deviations. ^bIn cyclohexane (ref 16a). ^cIn cyclohexane (ref 12). ^dIn decalin (this work). ^eMean of two values for $[\text{L}] = 0.4$ M. ^fIn xylene. Values of k_a and k_b estimated by fitting data in ref 19 to eq 3.

in $[\text{PPh}_3]$ would be expected to decrease the rate, yet no such decrease is observed when $[\text{PPh}_3]$ is almost doubled to 0.1 M. It was also found that reaction with $[\text{C}_2\text{H}_2\text{Cl}_4] = 0.1$ M, $[\text{complex}] = 1.4 \times 10^{-4}$ M, and in the absence of added PPh_3 , proceeds at just below the limiting rate. Competition of $\text{C}_2\text{H}_2\text{Cl}_4$ for the reactive intermediate is, therefore, slightly less than 100% successful. If the intermediate were $\text{Mn}_2(\text{CO})_8(\text{PPh}_3)$, formed by

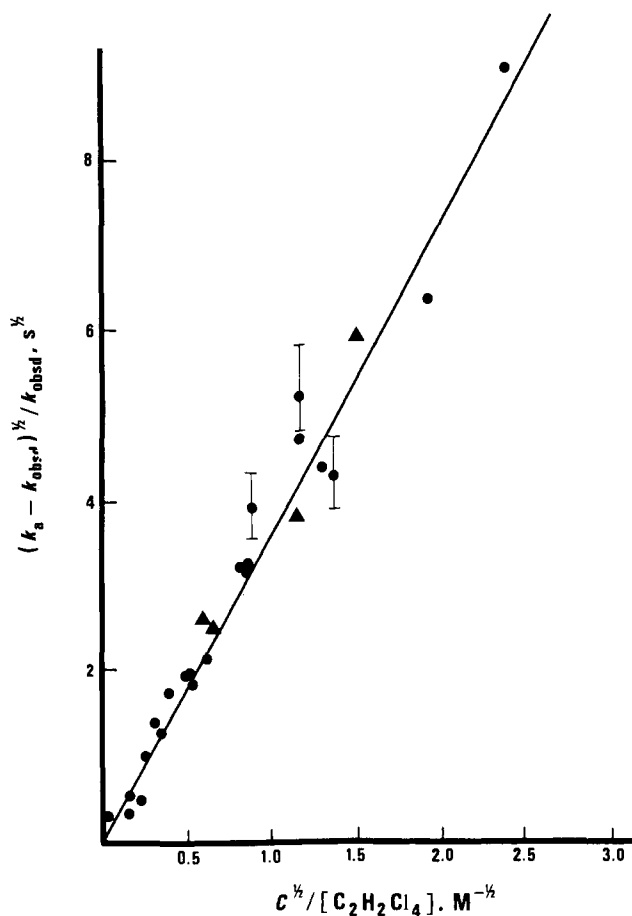
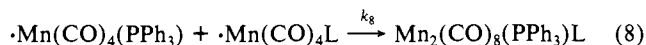
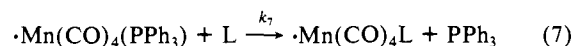
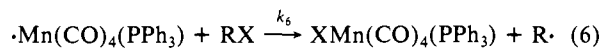
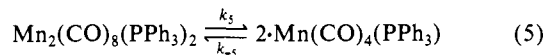


Figure 3. Dependence of $(k_a - k_{\text{obsd}})^{1/2} / k_{\text{obsd}}$ on $C^{1/2} / [\text{C}_2\text{H}_2\text{Cl}_4]$ for reaction at 49.9 °C with $10^4 k_a = 28.5 \text{ s}^{-1}$. (●) Reaction under Ar, $10^3 [\text{C}_2\text{H}_2\text{Cl}_4] = 2.4 - 500 \text{ M}$, $10^6 C = 3.5 - 334 \text{ M}$, $[\text{PPh}_3] = 0.06 \text{ M}$. (▲) Reaction under CO, $10^3 [\text{C}_2\text{H}_2\text{Cl}_4] = 12 - 30 \text{ M}$, $10^6 C = 188 - 332 \text{ M}$, $[\text{PPh}_3] = 0.10 \text{ M}$. Error bars exemplify uncertainties of $\pm 7.6\%$ in k_{obsd} , the value found for the probable error in an individual determination of k_{obsd} .

PPh_3 dissociation, then even the very small amount of PPh_3 released from the complex must be sufficient to compete detectably with $\text{C}_2\text{H}_2\text{Cl}_4$ for this intermediate. Addition of substantial further amounts of PPh_3 would be expected to decrease the rate greatly yet this is not observed. Thus, the values of $10^4 k_{\text{obsd}}$ when the concentration of added PPh_3 was 0, 0.06, 0.12, and 0.18 M were 28.6, 27.4, 28.6, and 28.5 s^{-1} , respectively. Exactly similar arguments to those above can be applied in rejecting the possibility of a CO dissociative mechanism. Experiments in the presence of added CO were carried out in the presence of sufficient PPh_3 to prevent displacement of this ligand from the complex at any stage of the reaction. No decrease in rate is observed when reactions were carried out under CO in place of Ar, so it can therefore be concluded that *rate determining dissociative processes play no detectable part in these reactions*.^{16b}

The rate equations shown in eq 3 and 4 have been shown^{3,12} to be characteristic of the mechanisms shown in eq 5–8, and the data are, therefore, in very good accord with these mechanisms. Reaction 6 is a second-order halogen-transfer step and (7) is an associative substitution reaction of a type that is now becoming quite common for 17-electron metal-centered radicals.^{12,18} The fate of the alkyl radicals in reaction 6 is not known in this case, but reactions such as (6) have been shown to occur after photo-



chemically induced homolysis of many such complexes without the radicals affecting the kinetic behavior.¹⁴ No difference in the form of the kinetics was observed when $\text{R} \cdot$ was $\cdot \text{C}_2\text{H}_2\text{Cl}_3$ or $\cdot \text{C}_{16}\text{H}_{33}$, nor were the limiting rates dependent on the nature of $\text{R} \cdot$. It is therefore most unlikely that the radicals $\text{R} \cdot$ play any role in the mechanism. According to this scheme, k_a can be equated with k_5 for all reactions and k_b can be equated with $4k_{-5}/k_6^2$ for reactions with the halocarbons¹ and to k_{-5}/k_7^2 for substitution reactions.¹² The factor of 4 is missing from the latter fraction because reaction 8 leads to a dinuclear product whereas (6) leads to a mononuclear one.

The Significance of the Limiting Rate Constant, k_a . The preceding analysis would be very satisfactory were it not for the fact that reaction with $\text{P}(\text{O}i\text{Pr})_3$ according to eq 1 is also in excellent quantitative agreement¹² with the mechanism described by eq 5, 7, and 8 but with the important difference that the value of the limiting rate constant, k_a , is substantially lower than that for reactions with the other six reactants mentioned above.^{13,16a} Reaction with CO proceeds to form $\text{Mn}_2(\text{CO})_9(\text{PPh}_3)$ with a value of k_a exactly equal to the low value shown by $\text{P}(\text{O}i\text{Pr})_3$.^{12,16a} This significant difference was implicit (Table I) in the data obtained by Wawersik and Basolo¹⁹ for substitution reactions of $\text{Mn}_2(\text{CO})_8(\text{PPh}_3)_2$ with $\text{P}(\text{O}i\text{Pr})_3$ and *P-n*-Bu₃ and was later explicitly recognized after more detailed studies of reactions with $\text{P}(\text{O}i\text{Pr})_3$, CO, and O₂.^{12,16a} No satisfactory explanation for this difference was found on the basis of the data then available.^{16a}

We have studied the source of this difference in the following way. Reactions with $\text{C}_2\text{H}_2\text{Cl}_4$ were carried out under an atmosphere of CO and in the absence of PPh_3 . Under these conditions the reactions proceeded to at least the lower limiting rate. It was possible to study the way in which this rate was enhanced by added $\text{C}_2\text{H}_2\text{Cl}_4$, and also the way in which the enhanced rate was dependent on C . The value of k_{obsd} was found to increase with $[\text{C}_2\text{H}_2\text{Cl}_4]$ from the lower limiting value characteristic of reaction with CO alone to that characteristic of $\text{C}_2\text{H}_2\text{Cl}_4$ alone at high $[\text{C}_2\text{H}_2\text{Cl}_4]$ (Figure 4). As the rates increased so the nature of the products changed from $\text{Mn}_2(\text{CO})_9(\text{PPh}_3)$ alone to $\text{C}(\text{Mn}(\text{CO})_4(\text{PPh}_3))_2$ alone via mixtures containing increasing proportions of the latter. This shows clearly that there must be two parallel paths, I and II, available for reaction. The reactants CO and $\text{P}(\text{O}i\text{Pr})_3$ can participate in only one of these, with a limiting rate governed by k_{11} and equal to the lower value of k_a in Table I. The reactants $\text{P}(\text{O}Et)_3$, *P-n*-Bu₃, O₂, NO, $\text{C}_2\text{H}_2\text{Cl}_4$, and $\text{C}_{16}\text{H}_{33}\text{I}$ can participate in *both* paths, the second having a limiting rate constant, k_{11} , equal to the difference between the higher and lower values of k_a in Table I. The enhanced rate shows a dependence on C similar to that shown by path I, the value of k_{obsd} decreasing steadily with increasing C as shown in Figure 5. This decrease is also quantitatively in excellent accord with eq 3 (Figure 6), so we are in the unusual position of having two distinct reaction paths both of which follow exactly the same rate equation.

Reaction Including Induced Homolysis. This kinetic behavior leads us to believe that reversible fragmentation must still be a feature of path II since it is a process that is essential for the type of [complex] dependence observed, particularly in view of the fact that ligand dissociation can be ruled out (see above). However, spontaneous homolysis has already been proposed for one of the paths so we find it necessary to postulate that the other involves some form of *induced* homolysis. A suggestion that fits with all the results is shown in Scheme I. This applies specifically to

(18) (a) Fox, A.; Malito, J.; Poë, A. J. *J. Chem. Soc., Chem. Commun.* **1981**, 1052. (b) McCullen, S. B.; Walker, H. W.; Brown, T. L. *J. Am. Chem. Soc.* **1982**, *104*, 4007–4008. (c) Poë, A. J. *Transition Met. Chem. (Weinheim, Ger.)* **1982**, *7*, 65–69. (d) Yesaka, H.; Kobayoshi, T.; Yasufuku, K.; Nagakuru, S. *J. Am. Chem. Soc.* **1983**, *105*, 6249–6252. (e) Hepp, A. F.; Wrighton, M. S. *Ibid.* **1983**, *105*, 5934–5935. (f) Shi, Q. Z.; Richmond, T. G.; Troglor, W. C.; Basolo, F. *Ibid.* **1982**, *104*, 4032–4034; **1984**, *106*, 71–80.

(19) Wawersik, H.; Basolo, F. *Inorg. Chim. Acta* **1969**, *3*, 113–120.

Scheme I

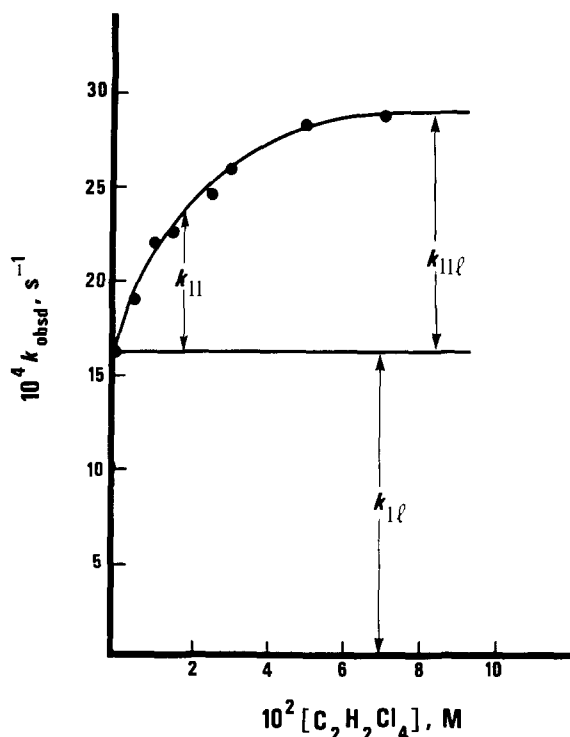
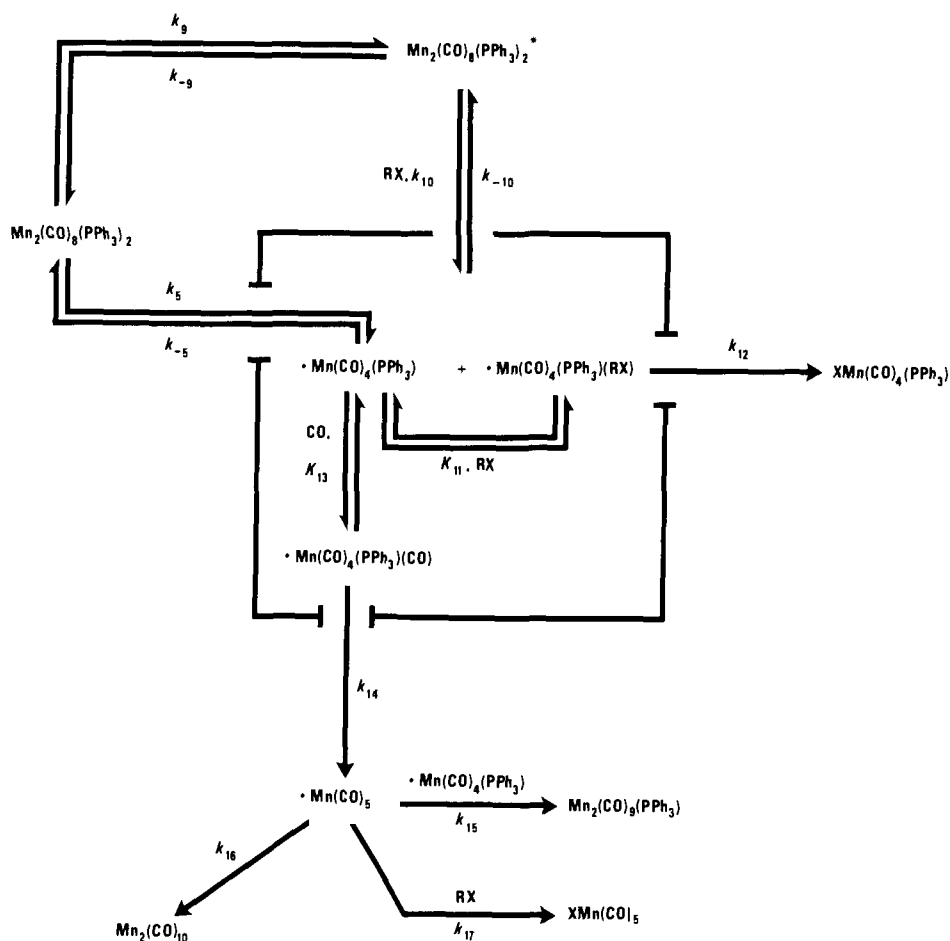


Figure 4. Dependence of k_{obsd} on $[\text{C}_2\text{H}_2\text{Cl}_4]$ for reaction at 49.9 °C under CO. $[\text{PPh}_3] = 0$. $C = (2.2 \pm 0.5) \times 10^{-4}$ M except for $[\text{C}_2\text{H}_2\text{Cl}_4] = 0$ when it is 5.9×10^{-4} M. k_{11} is the limiting rate constant for reaction with CO or $\text{C}_2\text{H}_2\text{Cl}_4$ by path I. k_{11} is the rate constant for reaction with $\text{C}_2\text{H}_2\text{Cl}_4$ by path II and increases to a limiting value, k_{11} , such that $k_{11} + k_{11l} =$ the higher value of k_a shown in Table I, k_{11} being equal to the lower value.

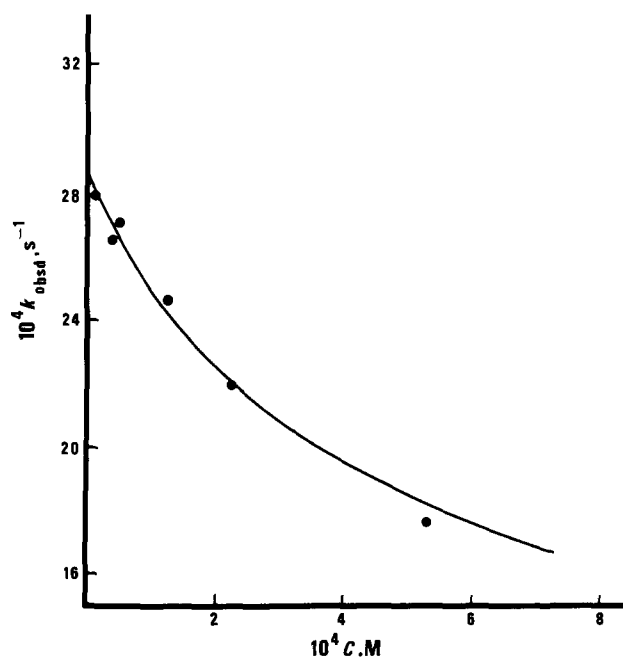


Figure 5. Dependence of k_{obsd} on C for reaction with $\text{C}_2\text{H}_2\text{Cl}_4$ under CO at 49.9 °C. $[\text{C}_2\text{H}_2\text{Cl}_4] = 0.01$ M, $[\text{PPh}_3] = 0$. The continuous line is calculated according to parameters obtained from Figure 6.

reactions with alkyl halides, either in the presence of CO or not, but it can easily be modified to account for reactions with the other reagents that have been used. Reaction numbers are indicated by the subscripts to the rate or equilibrium constants. For reasons that will be discussed below, the species enclosed by the rectangle are considered to be in labile equilibrium with each other but

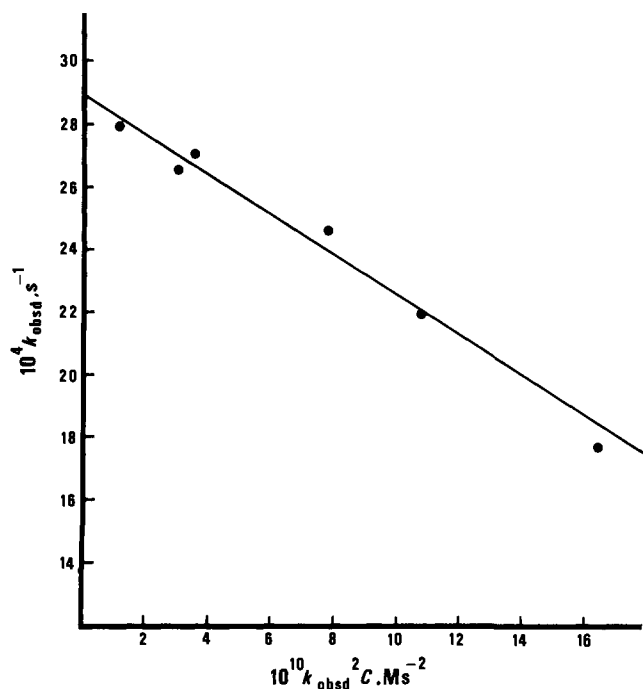


Figure 6. Dependence of k_{obsd} on $k_{\text{obsd}}^2 C$ for reaction with $C_2H_2Cl_4$ under CO at 49.9 °C. $[C_2H_2Cl_4] = 0.01$ M. Deviations of the points from the straight line lead to a probable error of $\pm 3.3\%$ for an individual determination of k_{obsd} .

reactions leading in and out of the rectangle are relatively very much slower.

$\cdot Mn(CO)_4(PPh_3)$ radicals are generated reversibly, as discussed above, by reaction 5. They react rapidly and reversibly to form the adducts $\cdot Mn(CO)_4(PPh_3)(RX)$ and, if CO is present, $\cdot Mn(CO)_4(PPh_3)(CO)$. These are 6-coordinate 19-electron radicals with the added molecules presumably being attached (via the X or C atoms) to the half-empty orbital that protrudes out of the square base of the square-based pyramidal $\cdot Mn(CO)_4(PPh_3)$.²⁰ These 19-electron radicals are of a type that is becoming quite widely recognized as being necessarily involved as intermediates in bimolecular substitution or oxidation reactions of 5-coordinate 17-electron metal centered radicals.^{18a-e} Similar radicals have been shown to play an essential role in photochemical disproportionations of some metal-metal bonded carbonyls.²¹ Some 19-electron carbonyl radicals have also been isolated.²²

$\cdot Mn(CO)_4(PPh_3)(RX)$ reacts slowly to form $XMn(CO)_4(PPh_3)$ via halogen atom transfer, reaction 6 above having been represented in Scheme I by the sequence (11) and (12). $\cdot Mn(CO)_4(PPh_3)(CO)$ undergoes a slow ligand interchange to form $\cdot Mn(CO)_5$, and this reacts predominantly with $\cdot Mn(CO)_4(PPh_3)$ to form $Mn_2(CO)_9(PPh_3)$, rather than with another $\cdot Mn(CO)_5$ to form $Mn_2(CO)_{10}$ via reaction 16. This combination of unlike radicals is also a feature of reactions with $P(OPh)_3$, $P(OEt)_3$, and $P-n-Bu_3$ and has been commented on before.⁷ A similar observation is that a significant product in the photochemically induced substitution of CO into $Mn_2(CO)_8(P-n-Bu_3)_2$ is $Mn_2(CO)_9(P-n-Bu_3)$.²³ This reaction is also believed to proceed via homolysis. These observations have to be ascribed to a combination of effects: the relative rate constants for radical dimerizations, the rates of the substitution reactions of the radicals, and the relative steady-state concentrations of the radicals.^{7,23} Thus, if $[\cdot Mn(CO)_5]$ is much smaller than $[\cdot Mn(CO)_4(PPh_3)]$ it is much more likely to react with the latter than with another $\cdot Mn(CO)_5$.

No $XMn(CO)_5$ is observed as a product of reaction with RX under CO, and reaction 17 is therefore unimportant. This must be due to the fact that, at low [RX] when most $\cdot Mn(CO)_5$ is formed, reaction with $\cdot Mn(CO)_4(PPh_3)$ turns out to be more probable. On the other hand, when [RX] is high and RX more likely to react with $\cdot Mn(CO)_5$, less $\cdot Mn(CO)_5$ is formed because of the preponderance of reactions 11 and 12 under those conditions.

These considerations apply to the formation of products via initial spontaneous homolysis. However, the intermediates $\cdot Mn(CO)_4(PPh_3)$ and $\cdot Mn(CO)_4(PPh_3)(RX)$ are, for the kinetic reasons outlined above, postulated to be formed as well by an alternative reversible fragmentation process. This involves initial reversible formation of a reactive isomeric form of $Mn_2(CO)_8(PPh_3)_2$ that is susceptible to reversible fragmentation when attacked by RX or any of the more reactive reagents. The reactive isomer is designated as $Mn_2(CO)_8(PPh_3)_2^*$, and the reversibility of its fragmentation is required by the nature of the [complex] dependence shown in Figures 5 and 6. This reversibility of the fragmentation also requires the products to be one $\cdot Mn(CO)_4(PPh_3)$ and one $\cdot Mn(CO)_4(PPh_3)(RX)$, and not simply two $\cdot Mn(CO)_4(PPh_3)$ radicals and a free RX molecule. In the latter case the reverse of reaction 10 would be trimolecular and hence very improbable.

The fragmentation cannot be induced by direct attack of RX on $Mn_2(CO)_8(PPh_3)_2$. If this occurred then either there would be no limiting rates approached at high [RX] or limiting rates would have to be reached by 100% adduct formation in a rapid preequilibrium. No spectroscopic evidence for such a preequilibrium is apparent, nor would it be expected that adducts containing as diverse species as O_2 , NO, *P-n-Bu_3*, $C_2H_2Cl_4$, etc., would all undergo fragmentation at the same rate, yet the data in Table I show that the limiting rates for all these reagents are essentially identical. It is, therefore, necessary to conclude that fragmentation is induced by reagent attack on the reversibly formed reactive isomer $Mn_2(CO)_8(PPh_3)_2^*$ as in steps 9 and 10, the products of which react exactly as already described.

Scheme I is thus capable of representing qualitatively all the main features of the reactions. Much more important, however, is the excellent quantitative fit that can be obtained. Allowing for the fact that reactions 16 and 17 can be neglected for reasons already discussed, the scheme leads to the rate equation shown in alternative forms in eq 18–20. Equation 19 is a rearranged

$$k_{\text{obsd}} = k_5 + k_9 - (k_{-5} + k_{-9}k_{-10}K_{11}/k_{10})k_{\text{obsd}}^2 C / \{0.5K_{11}k_{12}[RX] + K_{13}k_{14}[CO]\}^2 \quad (18)$$

$$f = k_{\text{obsd}} / (k_5 + k_9 - k_{\text{obsd}})^{1/2} = \{0.5K_{11}k_{12}[RX] + K_{13}k_{14}[CO]\} / C^{1/2} (k_{-5} + k_{-9}k_{-10}K_{11}/k_{10})^{1/2} \quad (19)$$

$$= \{0.5K_{11}k_{12}[RX] + K_{13}k_{14}[CO]\} / C^{1/2} \{k_{-5}(1 + k_9/k_5)\}^{1/2} \quad (20)$$

form of eq 18, and eq 20 takes account of the fact that $(k_5/k_{-5})K_{11} = (k_9/k_{-9})(k_{10}/k_{-10})$ so that $k_{-9}k_{-10}K_{11}/k_{10} = k_{-5}k_9/k_5$. Under the conditions used here, reaction 14 is irreversible and each time $\cdot Mn(CO)_5$ is formed reaction 15 follows. The rate constant k_{15} does not, therefore, appear in eq 18. Reactions 11 and 13 are postulated to be labile equilibria because they involve simple adduct formation with formation of relatively weak bonds. The radicals within the rectangle can, therefore, be treated as a single steady-state intermediate assemblage that is formed slowly by reactions 5 and 10 and lost slowly by the reverse of those reactions and by reactions 12 and 14. The concentration of the assemblage is given in terms of the total concentration of pairs of Mn atoms that it contains so that one pair is formed by reactions 5 and 10, one lost by reaction 14, and half a pair lost by reaction 12. This is the source of the factor 0.5 before k_{14} in eq 18 and 19. The derivations of the rate equations are shown in the Appendix where it can be seen that the particular form of eq 18 assumes that $k_{10}[RX] \gg k_{-9}$. This is required by the form of the kinetics. It does not simply imply that reaction by steps 9 and 10 always proceeds at rates governed by k_9 . k_{-10} can be comparable to

(20) Kidd, D. R.; Cheng, C. P.; Brown, T. L. *J. Am. Chem. Soc.* **1978**, *100*, 4103–4106.

(21) Stiegman, A. E.; Tyler, D. R. *Inorg. Chem.* **1984**, *23*, 527–529 and references therein. Goldman, A. S.; Tyler, D. R. *J. Am. Chem. Soc.* **1984**, *106*, 4066–4067.

(22) Maroney, M. J.; Troglor, W. C. *J. Am. Chem. Soc.* **1984**, *106*, 4144–4151.

(23) Kidd, D. R.; Brown, T. L. *J. Am. Chem. Soc.* **1978**, *100*, 4095–4103.

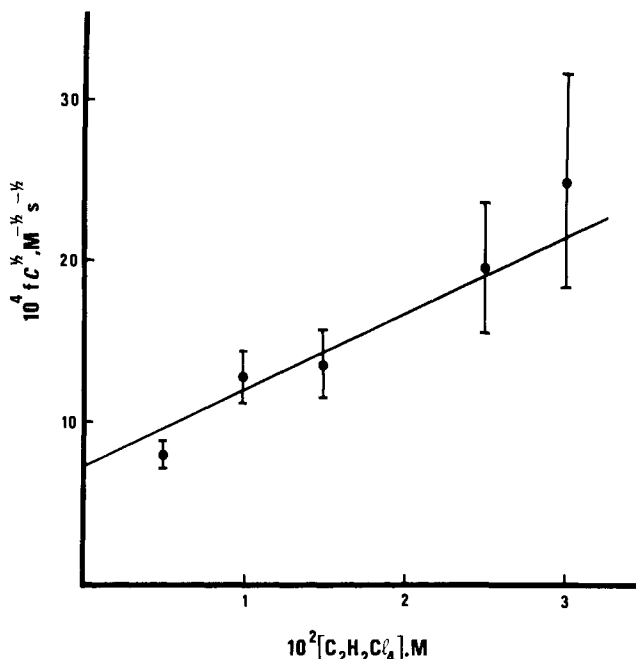


Figure 7. Dependence of $fC^{1/2}$ on $[C_2H_2Cl_4]$ for reaction under CO at 49.9 °C. $10^4C = 2.2 \pm 0.5$ M; $[PPh_3] = 0$. Error bars exemplify the effect of an uncertainty of $\pm 5\%$ in k_{obsd} . Deviation of the points from the straight line leads to a probable error of $\pm 3.8\%$ for an individual determination of k_{obsd} .

$k_{10}[RX]$ so that the *net* loss of $Mn_2(CO)_8(PPh_3)_2^*$ by reaction 10 is not necessarily much faster than its loss by the reverse of (9).

The fact that eq 18 has exactly the same form as eq 3 when $[RX]$ and $[CO]$ are constant conforms to the good linearity of the plot in Figure 6. The gradient has been used to calculate the smooth curve shown in Figure 5, and the intercept of 29.0 ± 0.5 s^{-1} is indistinguishable from the weighted mean of 28.85 ± 0.19 s^{-1} for the higher values of 10^4k_a at 49.9 °C in Table I found in this work. The probable error of an individual measurement of k_{obsd} , estimated from the residuals for the data in Figure 5, is $\pm 3.3\%$ so the fit of these data is very good indeed. The dependence of k_{obsd} on $[RX]$, for reactions under CO, can most conveniently be analyzed in terms of eq 20. A plot of $fC^{1/2}$ against $[RX]$ for $10^4C = 2.2 \pm 0.5$ M is shown in Figure 7 and conforms well to eq 20. Deviations of the data from the line drawn lead to an estimate of $\pm 3.8\%$ for the probable error in k_{obsd} .

All the data for these reactions under CO can be used in a least-squares analysis of the dependence of $fC^{1/2}$ on $[C_2H_2Cl_4]$. The data are shown in Table II together with values calculated according to the least-squares parameters. The probable error for an individual determination of k_{obsd} is $\pm 8.6\%$, but this reduced to $\pm 4.8\%$ if one point is neglected. The quantitative fit of all the data with the rate equations predicted by Scheme I is, therefore, excellent, and the scheme accounts precisely, and in the simplest way possible, for the nature of the products of the reactions and for all the kinetics.

The Spontaneous Homolysis Path. The situation when only one path is being followed, as exemplified by reaction with $P(OPh)_3$ or CO, must involve reaction via eq 5, 7, and 8, i.e., initial spontaneous homolysis. We know that k_5 and k_9 are of comparable magnitude so that $\cdot Mn(CO)_4(PPh_3)$ is formed at significant rates by spontaneous homolysis. Since it is an intermediate common to both paths it is not possible for it to be formed only by induced homolysis and not by reaction 5. On the other hand, reaction via (5) can occur as the only path even though k_9 is significant compared with k_5 . This is possible provided that $Mn_2(CO)_8(PPh_3)_2^*$ does not undergo fragmentation when attacked by CO or $P(OPh)_3$, i.e., reaction 10, with RX replaced by CO or $P(OPh)_3$, involves an insurmountable barrier. In this case, every time that reaction 9 occurs, the reverse reaction, governed by k_{-9} , always

Table II. Observed^a Rate Constants for Reaction of $Mn_2(CO)_8(PPh_3)_2$ with $C_2H_2Cl_4$ under CO

$10^4C, ^b$ M	$10^2[C_2H_2Cl_4],$ M	$10^4k_{obsd}^a,$ s^{-1}	$10^4k_{calcd}^c,$ s^{-1}	$\Delta, ^d$ %
5.29	1.0	17.6	17.8	-1.1
2.27	1.0	21.9	21.8	+0.5
1.32	1.0	24.6	23.9	+2.9
0.52	1.0	27.0	26.4	+2.3
0.45	1.0	26.5	26.7	-0.8
0.17	1.0	27.9	27.9	0
5.9	0	16.2	13.2	+22.7
1.74	0.5	18.9	21.3	-11.3
2.36	1.5	22.4	22.9	-2.2
2.58	2.5	24.5	24.5	0
2.36	3.0	25.8	25.4	+1.6
2.60	5.0	28.1	26.7	+5.2
2.70	7.0	28.6	27.4	+4.4

^a k_{obsd} is obtained from initial gradient of plots of $\ln(A_t - A_\infty)$ against t . ^b Initial concentration of complex. ^c Values of the rate constants calculated from a least-squares analysis of the dependence of $fC^{1/2}$ on $[C_2H_2Cl_4]$ using all the data. ^d Values of $100|k_{obsd} - k_{calcd}|/k_{calcd}$. $\{\Sigma\Delta^2/12\}^{1/2}$ leads to a probable error for k_{obsd} of 8.6% after allowance for the 10 degrees of freedom. Omission of the result with $\Delta = 22.7\%$ reduces the probable error to $\pm 4.8\%$.

negates it and reactions with CO and $P(OPh)_3$ proceed only via spontaneous homolysis.

Scrambling Reactions and Spontaneous Homolysis. The conclusion that spontaneous homolysis is occurring has been supported²⁴ by observations of the scrambling reaction shown in eq 21 ($Cy = C_6H_{11}$). This reaction was carried out in the absence

$$Mn_2(CO)_8(PPh_3)_2 + Mn_2(CO)_8(PCy_3)_2 \rightarrow 2Mn_2(CO)_8(PPh_3)(PCy_3) \quad (21)$$

of light and led to an equilibrium mixture of the three complexes. The reaction was not affected by the presence of added PPh_3 or PCy_3 . This shows²⁴ that phosphine dissociation does not play a role in the scrambling process. Although the spectroscopic changes were not suitable for obtaining good kinetic or equilibrium data, the initial rates at 40 °C were close to those for homolysis of $Mn_2(CO)_8(PPh_3)_2$. The rate of homolysis of $Mn_2(CO)_8(PCy_3)_2$ is known²⁴ to be much greater than that of $Mn_2(CO)_8(PPh_3)_2$ so that homolysis of the latter would be expected to be rate determining. The precision was unfortunately not good enough to show whether the rates were governed by k_{11} .

We have also studied the scrambling reaction shown in eq 22. Figure 8 shows the changes in the IR spectra observed when the reaction was carried out in decalin at 49.9 °C in the dark and

$$Mn_2(CO)_8(P-n-Bu_3)_2 + Mn_2(CO)_8(PPh_3)_2 \rightarrow 2Mn_2(CO)_8(PPh_3)(P-n-Bu_3) \quad (22)$$

with approximately equal initial concentrations of the two complexes. The bands at 1960 and 1950 cm^{-1} are due respectively to $Mn_2(CO)_8(PPh_3)_2$ and $Mn_2(CO)_8(P-n-Bu_3)_2$. Both decrease steadily in intensity while a band at 1955 cm^{-1} grows. The spectra show good isosbestic points over most of the reaction which is therefore quite clean. The reaction is unaffected by the presence of free PPh_3 which would suppress any dissociation of PPh_3 from $Mn_2(CO)_8(PPh_3)_2$. We have also shown PPh_3 to be incapable of displacing $P-n-Bu_3$ from $Mn_2(CO)_8(P-n-Bu_3)_2$ under these conditions. Phosphine dissociation does not, therefore,²⁴ provide a reaction path for reaction 22, and we conclude that it proceeds via spontaneous homolysis. In this case the rate is again controlled by the slower homolysis process, i.e., that of $Mn_2(CO)_8(P-n-Bu_3)_2$.¹³

Nature of the Reactive Isomer $Mn_2(CO)_8(PPh_3)_2^*$. The scheme involving induced homolysis closely resembles the initial stages of the chain reaction of $P-n-Bu_3$ or PPh_3 with $Co_2(CO)_8$ to form $[Co(CO)_3L_2^+][Co(CO)_4^-]$.²⁵ The main difference is that the adduct $Co_2(CO)_8L$ is formed by direct attack rather than via initial

(24) Poë, A. J.; Sekhar, C. V. *J. Chem. Soc., Chem. Commun.* **1983**, 566-567.

(25) Absi-Halabi, M.; Atwood, J. D.; Forbus, N. P.; Brown, T. L. *J. Am. Chem. Soc.* **1980**, *102*, 6248-6254.

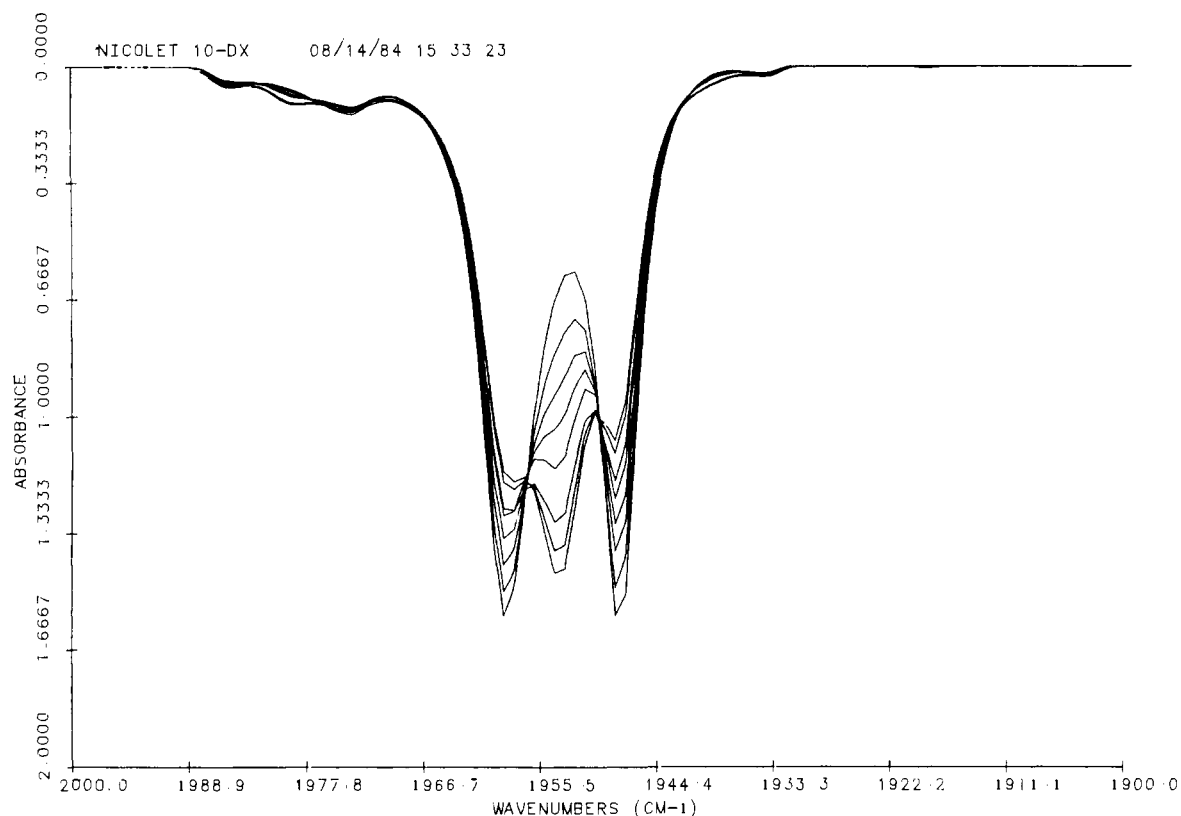
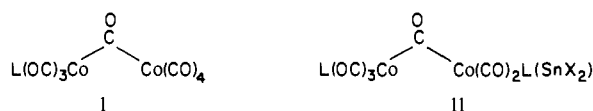
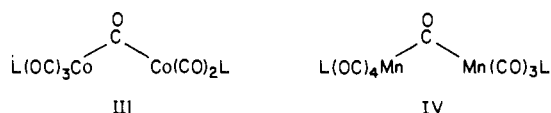


Figure 8. Changes in the IR spectra taken during the scrambling reaction of a mixture of $\text{Mn}_2(\text{CO})_8(\text{PPh}_3)_2$ ($\nu_{\text{CO}} = 2060 \text{ cm}^{-1}$) and $\text{Mn}_2(\text{CO})_8(\text{P-}n\text{-Bu}_3)_2$ ($\nu_{\text{CO}} = 2050 \text{ cm}^{-1}$) in decalin. The final spectrum is that of an equilibrium mixture of $\text{Mn}_2(\text{CO})_8(\text{PPh}_3)(\text{P-}n\text{-Bu}_3)$ ($\nu_{\text{CO}} = 2055 \text{ cm}^{-1}$) and unreacted unmixed complexes. The IR spectra were measured with a Nicolet 10DX FTIR spectrophotometer.

isomerization. $\text{Co}_2(\text{CO})_8\text{L}$ was formulated as I. This is an exact analogue of II which was proposed²⁶ as the intermediate in the



insertion of SnX_2 into $\text{Co}_2(\text{CO})_6\text{L}_2$ ($\text{L} = \text{P-}n\text{-Bu}_3$). When $\text{X} = \text{Br}$, II was formed by direct attack on the complex but, when $\text{X} = \text{Cl}$, isomerization of $\text{Co}_2(\text{CO})_6\text{L}_2$ to III was required before formation of II. It therefore seems not unreasonable to propose



that $\text{Mn}_2(\text{CO})_8(\text{PPh}_3)_2^*$ has the form shown in IV and that attack at the vacant coordination site on the right-hand Mn atom can lead to fragmentation provided the attacking group is reactive enough. We have to conclude that CO and $\text{P}(\text{O}^i\text{Ph})_3$ are not reactive enough to lead to fragmentation so that substitution via induced homolysis is not possible for these weak nucleophiles. All the other reactants are either stronger nucleophiles or are capable of inducing electron-transfer reactions of some kind. The formulation of reactive intermediates with two metals joined only by a bridging carbonyl has a long history^{26,27} and recently growing^{1,25,28} popularity since they provide a convenient rationale for

many reactions. Intermediates containing such a bridging carbonyl are believed to have been characterized spectroscopically,²⁹ and an analogue containing a Ph_2Ge bridge has been implicated in reactions of $\text{Co}_2(\text{CO})_7\text{GePh}_2$.³⁰

Activation Parameters. Now that the assignment of the limiting rate constants for reaction with CO and $\text{P}(\text{O}^i\text{Ph})_3$ to k_5 has been confirmed, the corresponding activation parameters^{16a} $\Delta H_5^\ddagger = 28.01 \pm 0.20 \text{ kcal mol}^{-1}$ and $\Delta S_5^\ddagger = 15.4 \pm 0.6 \text{ cal K}^{-1} \text{ mol}^{-1}$ can be assigned to the spontaneous homolysis process. Previously it was not clear whether the parameters for reaction with CO or with O_2 were the appropriate ones.^{16a} Activation parameters for the O_2 -induced homolysis path,^{16b} controlled by k_9 , can now be calculated. The average limiting rate constant for reaction with CO at a given temperature was subtracted from the rate constants for reaction with O_2 at that temperature.^{16a} The values for k_9 so obtained were used in a least-squares analysis of the dependence of $\ln(k_9/T)$ on $1/T$ to give $\Delta H_9^\ddagger = 29.49 \pm 0.33 \text{ kcal mol}^{-1}$ and $\Delta S_9^\ddagger = 19.6 \pm 1.1 \text{ cal K}^{-1} \text{ mol}^{-1}$.

Rate Constants for Reactions of $\cdot\text{Mn}(\text{CO})_4(\text{PPh}_3)$. Inspection of eq 3 and 18–20 shows that the second-order rate constants $K_{11}k_{12}$ for the halogen-transfer reaction of RX with $\cdot\text{Mn}(\text{CO})_4(\text{PPh}_3)$ are given by $2\{k_{-5}(1 + k_9/k_5)/k_b\}^{1/2}$ when the reactions are carried out under argon. Similarly, the rate constant for the substitution reaction of $\text{P}(\text{OEt})_3$ with $\cdot\text{Mn}(\text{CO})_4(\text{PPh}_3)$ is given by $\{k_{-5}(1 + k_9/k_5)/k_b\}^{1/2}$, the factor of 2 no longer being present because of the statistical effects discussed above. Since reaction 9 is not made use of by $\text{P}(\text{O}^i\text{Ph})_3$, the rate constant for its substitution reaction with $\cdot\text{Mn}(\text{CO})_4(\text{PPh}_3)$ is given simply by $(k_{-5}/k_b)^{1/2}$.

Values of k_9/k_5 are known, and a value $k_{-5} = 1 \times 10^7 \text{ M}^{-1} \text{ s}^{-1}$ has been obtained by direct measurement of $\cdot\text{Mn}(\text{CO})_4(\text{PPh}_3)$ dimerization in hexane at 25 °C after flash photolysis of Mn_2 -

(26) Barrett, P. F.; Poë, A. J. *J. Chem. Soc. A* **1968**, 429–433.
 (27) Breitschaft, S.; Basolo, F. *J. Am. Chem. Soc.* **1966**, *88*, 2702–2706.
 (28) (a) DeWit, D.; Fawcett, J. P.; Poë, A. J.; Twigg, M. V. *Coord. Chem. Rev.* **1972**, *8*, 82–85. (b) Basato, M.; Poë, A. J. *J. Chem. Soc., Dalton Trans.* **1974**, 607–612. (c) Bryndza, H. E.; Bergman, R. G. *J. Am. Chem. Soc.* **1979**, *101*, 4766–4768. (d) Theopold, K. H.; Bergman, R. G., *Ibid.* **1980**, *102*, 5694–5695. (e) Theopold, K. H.; Bergman, R. G. *Organometallics* **1982**, *1*, 1571–1579. (f) Malito, J.; Markiewicz, S.; Poë, A. J. *Inorg. Chem.* **1982**, *21*, 4335–4337. (g) Desrosiers, M. F.; Ford, P. C. *Organometallics* **1982**, *1*, 1715–1716. (h) Stiegman, A. E.; Tyler, D. R., *J. Am. Chem. Soc.* **1982**, *104*, 2944–2945. (i) Stiegman, A. E.; Tyler, D. R. *Acc. Chem. Res.* **1984**, *17*, 61–66.

(29) Tyler, D. R.; Schmidt, M. A.; Gray, H. B. *J. Am. Chem. Soc.* **1983**, *105*, 6018–6021; **1979**, *101*, 2753–2755.

(30) Basato, M.; Fawcett, J. P.; Fieldhouse, S. A.; Poë, A. J. *J. Chem. Soc., Dalton Trans.* **1974**, 1856–1859. Basato, M.; Fawcett, J. P.; Poë, A. J. *Ibid.* **1974**, 1350–1356.

Table III. Estimated^a Second-Order Rate Constants for Halogen Transfer to, or Displacement of PPh₃ from, $\cdot\text{Mn}(\text{CO})_4(\text{PPh}_3)$ in Decalin

<i>T</i> , °C	reactant	$10^{-2}k$, M ⁻¹ s ⁻¹
49.9	P(OPh) ₃ ^{b,c}	6.3 ± 0.7
	P(OEt) ₃ ^c	7.4 ± 0.2
	CO ^d	6.0 ± 1.2
	CO ^e	8.2 ± 0.8
	C ₂ H ₂ Cl ₄ ^d	4.1 ± 0.9
	C ₂ H ₂ Cl ₄ ^c	2.5 ± 0.2
39.9	C ₁₆ H ₃₃ I ^c	35.5 ± 1.0
	P(OPh) ₃ ^{b,c}	2.9 ± 0.1

^aSee text for details. Uncertainties are estimates of standard deviations that do not include any uncertainty in k_{-5} . The relative values of k are not affected by the uncertainty in k_{-5} . ^bIn cyclohexane. ^cFrom combination of values of k_{-5} (see text) and k_b in Table I. ^dFrom weighted least-squares analysis of all data for reaction with C₂H₂Cl₄ under CO. ^eFrom combination of gradients in Figures 3 and 6.

(CO)₈(PPh₃)₂.³¹ Assumption that $\Delta H_{-5}^{\ddagger} = \text{ca. } 3 \text{ kcal mol}^{-1}$ leads to a value of ca. $1.36 \times 10^7 \text{ M}^{-1} \text{ s}^{-1}$ for k_{-5} at 49.9 °C, and this is unlikely to be very different in decalin than in hexane. (This value of ΔH_{-5}^{\ddagger} leads to a value of $-16 \text{ cal K}^{-1} \text{ mol}^{-1}$ for ΔS_{-5}^{\ddagger} .) These values of k_{-5} lead to $\{k_{-5}(1 + k_9/k_5)\}^{1/2} = 4.73 \times 10^3 \text{ M}^{-1/2} \text{ s}^{-1/2}$ at 49.9 °C. Combination with the values of k_b in Table I allows estimates to be made of the various second-order rate constants for reactions with $\cdot\text{Mn}(\text{CO})_4(\text{PPh}_3)$, and these are shown in Table III. A value can also be estimated for reaction of P(OPh)₃ at 39.9 °C, and this allows values of $\Delta H^{\ddagger} = 16 \pm 2 \text{ kcal mol}^{-1}$ and $\Delta S^{\ddagger} = 3 \pm 7 \text{ cal K}^{-1} \text{ mol}^{-1}$ to be obtained for this reaction. The quoted uncertainties are related only to the precision of the two values for k_b given in Table I, and a value of half the uncertainty in ΔH_{-5}^{\ddagger} has to be added to give the total uncertainties. These are unlikely, therefore, to be much more than $\pm 3 \text{ kcal mol}^{-1}$ and $\pm 10 \text{ cal K}^{-1} \text{ mol}^{-1}$, respectively.

A value for the second-order rate constant for substitution by CO can be obtained from data for reaction with C₂H₂Cl₄ under CO. Since $K_{11}k_{12}$ is known from data for reaction with C₂H₂Cl₄ under Ar, the gradient of the plot in Figure 6 allows a value of $K_{13}k_{14}$ to be estimated, [CO] being taken to be $5.7 \times 10^{-3} \text{ M}$ at 49.9 °C in decalin.³² Inspection of eq 20 shows that values for $K_{11}k_{12}$ and $K_{13}k_{14}$ can be estimated quite independently, from the gradient and intercept, respectively, of the plot in Figure 7. These values are also given in Table III. The rate constants estimated for reaction with CO are in excellent agreement with each other, and those for reaction with C₂H₂Cl₄ are in quite good agreement allowing for the large uncertainty in the value based on Figure 7.

The uncertainties of the rate constants in Table III are based either on the uncertainties in the values of k_b shown in Table I or on the uncertainties estimated graphically from the plots in Figures 6 and 7. No allowance for the uncertainty in $k_{-5}^{1/2}$ has been included, but this is likely to be small and, in any case, does not affect the relative values of the rate constants.

The rate constants for substitution are not at all dependent on the nature of the nucleophile as would be expected for these fast reactions. Compensation of steric and electronic effects may occur. CO is a very weak nucleophile but is the smallest of those studied.³³ The value of ΔS^{\ddagger} for reaction with P(OPh)₃ is likely to be closer to the negative limit quoted because of the bimolecular nature of the reaction. In this case, ΔH^{\ddagger} would be ca. 13 kcal mol^{-1} which is only slightly lower than the values for substitution of P(OPh)₃ into Ru₃(CO)₁₂³⁴ or Co(CO)₃(NO).³⁵

The large value for k_b (Table I) for reaction of Mn₂(CO)₈-(PPh₃)₂ with P(OPh)₃ in xylene compared with that in cyclohexane is indicative of a pronounced solvent effect, though whether this is due to slower substitution or faster dimerization, or a combination of both, is not obvious.

The rate constant for Cl transfer from C₂H₂Cl₄ is considerably smaller than that for I transfer from C₁₆H₃₃I, as might be expected if C–X bond breaking is important. The rate constant for Cl transfer from C₂H₂Cl₄ to $\cdot\text{Mn}(\text{CO})_4(\text{PPh}_3)$ is much smaller than those for Cl transfer from CCl₄ to $\cdot\text{Mn}(\text{CO})_5$ at 25 °C in methanol³⁶ or cyclohexane.³⁷ It is not clear how much this is due to stronger C–Cl bonds in C₂H₂Cl₄ or to possible lower reactivity of $\cdot\text{Mn}(\text{CO})_4(\text{PPh}_3)$.

Implications of the Results. The results of this study have important general implications with regard to reactions of the dimetal decacarbonyls and their derivatives. They show that kinetic behavior previously^{1–4} thought to be uniquely assignable to spontaneous, reversible homolysis is in fact only a necessary and not sufficient indication of that mechanism. The same kinetic behavior can occur when the homolysis is induced by some suitably active reactant. A distinction is only possible if, as in this case, both paths can occur with some reactants but only one with others or if rates are known for scrambling reactions in the absence of any reactant capable of inducing homolysis.

In the case of the decacarbonyls, scrambling does not occur at rates consistent with spontaneous homolysis of the decacarbonyls themselves,^{8–10} and it was suggested⁹ that fragmentation occurs after CO dissociation. No kinetics of the scrambling reactions were obtained, but studies of the Mn₂(CO)₁₀–Re₂(CO)₁₀ scrambling reaction carried out subsequently in this laboratory¹¹ showed that it occurs via aggregation to tetranuclear intermediates rather than fragmentation of M₂(CO)₉ species. The suggestion that fragmentation follows CO dissociation was also adduced⁹ as a possible explanation of the kinetic results obtained for thermal decomposition of Mn₂(CO)₁₀² and Re₂(CO)₁₀³ in the presence of O₂. While it remains true that the results could now be explained by a mechanism in which O₂ induces fragmentation of reactive isomers of the decacarbonyls, it is also true that detailed quantitative studies of the effect of CO on these decompositions are required and such studies have been initiated.

As far as the disubstituted complexes, Mn₂(CO)₈L₂, are concerned we find that, when L = PPh₃, spontaneous homolysis and metal migration to form IV proceed at very similar rates. The activation enthalpy for spontaneous homolysis is slightly lower than that for metal migration, but the activation entropy is slightly less positive. On the basis of the fact that Mn₂(CO)₈(P-*n*-Bu₃)₂ also undergoes a scrambling reaction with Mn₂(CO)₈(PPh₃)₂, it has been suggested¹⁵ that all the complexes Mn₂(CO)₈L₂ (L = PPh(OMe)₂, PET₃, P-*n*-Bu₃, PPhEt₂, P(*p*-MeOC₆H₄), PPh₃, and PCy₃) undergo spontaneous homolysis so that the trend of substantially decreasing activation parameters along this series of complexes can be related to decreasing Mn–Mn bond strengths. This decrease can be ascribed to steric effects of the substituents.^{1,38} When L becomes small enough, spontaneous homolysis evidently becomes less favored so that some other path or paths are preferred for Mn₂(CO)₁₀. The kinetics of reaction with O₂^{2,39} and of substitution³⁹ suggest that both induced homolysis and CO dissociation paths may be available. It is not yet clear exactly how small L has to be for mechanistic changeover to occur. This will depend on the relative importance of steric effects in the various mechanisms, but one must conclude that they are more important for spontaneous homolysis.

Finally, the derivation of the data in Table III for bimolecular reactions of $\cdot\text{Mn}(\text{CO})_4(\text{PPh}_3)$ shows that relative rate constants can readily be obtained for such radicals by conventional thermal kinetic studies of spontaneous or induced homolysis, and absolute

(31) Walker, H. W.; Herrick, R. S.; Olsen, R. J.; Brown, T. L. *Inorg. Chem.* **1984**, *23*, 3748–3752.

(32) Basato, M.; Fawcett, J. P.; Poë, A. J. *J. Chem. Soc., Dalton Trans.* **1974**, 1350–1356.

(33) Tolman, C. A. *Chem. Rev.* **1977**, *77*, 313–348.

(34) Poë, A. J.; Twigg, M. V. *J. Chem. Soc., Dalton Trans.* **1974**, 1860–1866.

(35) Thorsteinson, E. M.; Basolo, F. *J. Am. Chem. Soc.* **1966**, *88*, 3929–3936.

(36) Meckstroth, K. W.; Walters, R. T.; Waltz, W. L.; Wojcicki, A. *J. Am. Chem. Soc.* **1982**, *104*, 1842–1846.

(37) Calculated from data in ref 18d and 14c.

(38) Jackson, R. A.; Poe, A. J. *Inorg. Chem.* **1979**, *18*, 3331–3333.

(39) Haines, L. I. B.; Hopgood, D.; Poë, A. J. *J. Chem. Soc. A* **1968**, 421–428.

values can be obtained when radical dimerization rates are known from flash photolysis studies.³¹

Acknowledgment. We thank the Natural Sciences and Engineering Research Council, Ottawa, for support and Professor T. L. Brown for communicating his results to us prior to publication.

Appendix

Derivation of the Rate Equations. If $\cdot\text{Mn}(\text{CO})_4(\text{PPh}_3)$ is represented by A we have, for the reactions shown in Scheme I

$$R = -d[\text{A}_2]/dt = (k_5 + k_9)[\text{A}_2] - k_{-5}[\text{A}_2]^2 - k_{-9}[\text{A}_2^*] \\ = 0.5k_{12}[\text{A}(\text{RX})] + k_{14}[\text{A}(\text{CO})]$$

Since the radicals enclosed in the rectangle in Scheme I are considered to be in labile equilibrium with each other⁴⁰ we have

$$[\text{A}] = [\text{A}(\text{RX})]/K_{11}[\text{RX}] = [\text{A}(\text{CO})]/K_{13}[\text{CO}]$$

and

$$[\text{A}(\text{CO})] = K_{13}[\text{CO}][\text{A}(\text{RX})]/K_{11}[\text{RX}]$$

whence

$$R = [\text{A}(\text{RX})]\{0.5K_{11}k_{12}[\text{RX}] + K_{13}k_{14}[\text{CO}]\}/K_{11}[\text{RX}] = \\ a[\text{A}(\text{RX})]$$

and

$$[\text{A}]^2 = [\text{A}(\text{RX})]^2/K_{11}^2[\text{RX}]^2 = R^2/a^2K_{11}^2[\text{RX}]^2$$

Similarly, $[\text{A}][\text{A}(\text{RX})] = R^2/a^2K_{11}[\text{RX}]$ and

$$d[\text{A}_2^*]/dt =$$

$$k_9[\text{A}_2] - \{k_{-9} + k_{10}[\text{RX}]\}[\text{A}_2^*] + k_{-10}[\text{A}][\text{A}(\text{RX})] = 0$$

i.e.

$$[\text{A}_2^*] = \{k_9[\text{A}_2] + k_{-10}R^2/a^2K_{11}[\text{RX}]\}/\{k_{-9} + k_{10}[\text{RX}]\}$$

(40) Rate equations so derived fit very well with the data, and we have not been able to derive rate equations without making this simplifying assumption.

whence

$$R = k_5[\text{A}_2] + k_9[\text{A}_2]\{1 - k_{-9}/(k_{-9} + k_{10}[\text{RX}])\} - \\ \{k_{-9}k_{-10}R^2/(k_{-9} + k_{10}[\text{RX}])a^2K_{11}[\text{RX}]\} - k_{-5}R^2/a^2K_{11}^2[\text{RX}]^2$$

Taking $k_{\text{obsd}} = R/[\text{A}_2] = R/C$ we have

$$k_{\text{obsd}} = k_5 + k_9k_{10}[\text{RX}]/(k_{-9} + k_{10}[\text{RX}]) - \\ \{k_{-9}k_{-10}/(k_{-9} + k_{10}[\text{RX}]) + k_{-5}/K_{11}[\text{RX}]\}k_{\text{obsd}}^2C/a^2K_{11}[\text{RX}]$$

When $k_{10}[\text{RX}] \gg k_{-9}$

$$k_{\text{obsd}} = k_5 + k_9 - (k_{-9}k_{-10}/k_{10} + k_{-5}/K_{11})k_{\text{obsd}}^2C/a^2K_{11}[\text{RX}]^2$$

which is identical with eq 18 when a is expressed in full.

An equation for substitution reactions in the absence of CO can be derived in exactly the same way. The reactions involving CO in Scheme I are ignored, and RX in reactions 10 and 11 is replaced by L. Reaction 12 then involves formation of $\cdot\text{Mn}(\text{CO})_4\text{L}$ from $\cdot\text{Mn}(\text{CO})_4(\text{PPh}_3)(\text{L})$ and is immediately followed by reaction with $\cdot\text{Mn}(\text{CO})_4(\text{PPh}_3)$ to form $\text{Mn}_2(\text{CO})_8(\text{PPh}_3)(\text{L})$. Thus, each time reaction 12 occurs two radicals are lost from the steady-state assemblage and $R = k_{12}[\cdot\text{Mn}(\text{CO})_4(\text{PPh}_3)(\text{L})]$, i.e., the statistical factor of 0.5 no longer appears as it did for reactions with RX. The rate equation obtained for substitution by combined spontaneous and induced homolysis is then easily shown to be

$$k_{\text{obsd}} = k_5 + k_9 - (k_{-5} + k_{-9}k_{-10}K_{11}/k_{10})k_{\text{obsd}}^2C/k_{12}^2K_{11}^2[\text{L}]^2$$

provided $k_{10}[\text{L}] \gg k_{-9}$, as before.

Registry No. $\text{Mn}_2(\text{CO})_8(\text{PPh}_3)_2$, 10170-70-4; CO, 630-08-0; $\text{P}(\text{O}^i\text{Ph})_3$, 101-02-0; O_2 , 7782-44-7; $\text{C}_{16}\text{H}_{33}\text{I}$, 544-77-4; $\text{C}_2\text{H}_2\text{Cl}_4$, 25322-20-7; $\text{P}-n\text{-Bu}_3$, 998-40-2; $\text{P}(\text{OEt})_3$, 122-52-1; NO, 10102-43-9; $\text{Mn}_2(\text{CO})_{10}$, 10170-69-1.

Supplementary Material Available: Tables of rate constants (4 pages). Ordering information is given on any current masthead page.

Fundamental Study of the Oxidation of Butane over Vanadyl Pyrophosphate

Marc A. Pepera, James L. Callahan, Michael J. Desmond,* Ernest C. Milberger, Patricia R. Blum, and Noel J. Bremer

Contribution from the Corporate Research Department of The Standard Oil Company, Cleveland, Ohio 44128. Received December 14, 1984

Abstract: The oxidation of butane as catalyzed by $\beta\text{-(VO)}_2\text{P}_2\text{O}_7$ was studied as a function of the separate catalyst oxidation and reduction steps. The vanadyl pyrophosphate was found to have a reversible oxidation capacity approaching one oxygen molecule per two surface vanadium centers. The reduction reaction of the catalyst surface was found to be first order in butane and the oxidation reaction was found to be first order in oxygen. These two reactions occur in distinct, separate steps, a behavior similar to that exhibited by catalysts which can utilize lattice oxygen from the bulk in oxidation reactions. Pulse studies over the catalyst, involving the use of ^2H - and ^{18}O -labeled compounds, revealed a very dynamic surface for $\beta\text{-(VO)}_2\text{P}_2\text{O}_7$ at 400 °C. All oxygen and hydrogen atoms in the surface layer were found to be in fast exchange relative to the time scale of the conversion of butane to maleic anhydride and combustion products. Experiments with deuterium-labeled butane revealed that the rate-controlling step for butane oxidation was the irreversible activation of a methylene carbon-hydrogen bond in butane on the catalyst surface. Vanadium(IV) sites on the catalyst surface are proposed to be responsible for both the chemisorption of oxygen and the activation of butane. The combination of a $\text{V(V)} \rightleftharpoons \text{V(IV)}$ couple and the dynamic nature of the surface layer are thought to be mechanistically important for the 14-electron oxidation of butane to maleic anhydride.

The petrochemical industry currently relies on unsaturated molecules obtained from the refining process to produce derivative chemicals. Recent efforts have been directed at the substitution of paraffinic molecules for the more valuable unsaturates in some of these processes. The challenge of activating a C-H bond at

a saturated carbon center with the conversions and selectivities required for an industrial process is a monumental one. Over the last decade, processes which form maleic anhydride from the oxidation of butane have significantly displaced previous technology which relied on benzene. This conversion represents a very